UNCLASSIFIED

NAVAL AIR WARFARE CENTER AIRCRAFT DIVISION
PATUXENT RIVER, MARYLAND

TECHNICAL REPORT

REPORT NO: NAWCADPAX/TR-2001/177

MICROSTRUCTURAL EFFECT ON FATIGUE OF 7075 ALUMINUM ALLOY

by

Eun U. Lee
Henry C. Sanders

8 January 2002

20020214 070

Approved for public release; distribution is unlimited.

UNCLASSIFIED

DEPARTMENT OF THE NAVY
NAVAL AIR WARFARE CENTER AIRCRAFT DIVISION
PATUXENT RIVER, MARYLAND

NAWCADPAX/TR-2001/177
8 January 2002

MICROSTRUCTURAL EFFECT ON FATIGUE OF 7075 ALUMINUM ALLOY

by

Eun U. Lee
Henry C. Sanders

RELEASED BY:

W- Fragin for Dale Moore

DALE MOORE / CODE 4.3.4 / DATE
Director, Materials Competency
Naval Air Warfare Center Aircraft Division

REPORT DOCUMENTATION PAGE			Form Approved OMB No. 0704-0188

1. REPORT DATE 8 January 2002	2. REPORT TYPE Technical Report	3. DATES COVERED
4. TITLE AND SUBTITLE Microstructural Effect on Fatigue of 7075 Aluminum Alloy		5a. CONTRACT NUMBER 5b. GRANT NUMBER 5c. PROGRAM ELEMENT NUMBER
6. AUTHOR(S) Eun U. Lee Henry C. Sanders		5d. PROJECT NUMBER 5e. TASK NUMBER 5f. WORK UNIT NUMBER
7. PERFORMING ORGANIZATION NAME(S) AND ADDRESS(ES) Naval Air Warfare Center Aircraft Division 22347 Cedar Point Road, Unit #6 Patuxent River, Maryland 20670-1161		8. PERFORMING ORGANIZATION REPORT NUMBER NAWCADPAX/TR-2001/177
9. SPONSORING/MONITORING AGENCY NAME(S) AND ADDRESS(ES) Naval Air Systems Command 47123 Buse Road Unit IPT Patuxent River, Maryland 20670-1547		10. SPONSOR/MONITOR'S ACRONYM(S) 11. SPONSOR/MONITOR'S REPORT NUMBER(S)
12. DISTRIBUTION/AVAILABILITY STATEMENT Approved for public release; distribution is unlimited.		
13. SUPPLEMENTARY NOTES		

14. ABSTRACT

This study was conducted to characterize the fatigue behavior of underaged and overaged 7075 aluminum alloy in vacuum of $4x10^{-8}$ torr. An emphasis was placed on clarifying the effects of different microstructures, arising from the underaging and overaging treatments, on the threshold fatigue crack growth (FCG). The FCG was measured under constant amplitude loading of stress ratios, ranging from 0.1 to 0.85, in vacuum of $4x10^{-8}$ torr. The result was analyzed in terms of threshold stress intensity range (ΔK_{th}) for FCG and maximum stress intensity (K_{max}). It was found that the underaging resulted in lower electrical conductivity, higher hardness, and greater resistance to threshold FCG than the overaging. This is attributable to the difference in microstructure.

15. SUBJECT TERMS

7075
Fatigue Crack Growth
Aluminum Alloy

16. SECURITY CLASSIFICATION OF:			17. LIMITATION OF ABSTRACT	18. NUMBER OF PAGES	19a. NAME OF RESPONSIBLE PERSON Eun U. Lee
a. REPORT	b. ABSTRACT	c. THIS PAGE			19b. TELEPHONE NUMBER (include area code)
Unclassified	Unclassified	Unclassified	SAR	34	(301)342-8069

Standard Form 298 (Rev. 8-98)
Prescribed by ANSI Std. Z39-18

SUMMARY

In order to establish the role of microstructure on fatigue in the absence of corrosion, the fatigue crack growth (FCG) behavior of underaged and overaged 7075 aluminum alloy was investigated in vacuum of 4×10^{-8} torr. The specimens were subjected to fatigue loading of constant amplitude with various stress ratios, ranging from 0.1 to 0.85, in vacuum of 4×10^{-8} torr. The measured FCG was analyzed in terms of two driving force parameters, threshold stress intensity range (ΔK_{th}) and maximum stress intensity (K_{max}). The result indicates that the underaged specimen has lower electrical conductivity, higher hardness, and greater resistance to threshold FCG than the overaged one. This is attributed to the different microstructures, produced by the different aging treatments, and the resultant different slip modes, planar and wavy.

CONTENTS

ACKNOWLEDGMENTS

The authors would like to thank the Office of Naval Research (ONR) for sponsoring this work. Thanks are also due to Dr. A. K. Vasudevan of ONR and Professor Stefanie Tshegg of the Institute of Meteorology and Physics, Vienna, Austria, for providing the specimen materials and many valuable advices. Finally, thanks are due to Dr. Bhaskar Sarkar, Miss Veena Agarwala, Dr. Charles Lei, and Mr. Jack O'Brian of NAWCAD Patuxent River, Maryland (Code 4.3.4.2) for their preparation and examination of transmission electron microscope and optical micrographs and scanning electron microscope fractographs and measurement of electrical conductivity.

INTRODUCTION

It has been known that a microstructure plays a major role on the fatigue crack growth (FCG) behavior of a metallic material. There are various microstructural features that potentially affect the FCG. Grain and subgrain boundaries serve as barriers to the transmission of slip-band cracks, and constituent particles and hardening precipitates influence the FCG significantly.

A number of studies have been conducted to ascertain the effect of microstructure on the FCG in aluminum alloys (references 1 through 15). Underaging produces coherent precipitates, which are sheared by moving dislocations resulting in planar slip, along which a fatigue crack grows. Overaging produces incoherent precipitates, which are looped and bypassed by dislocations resulting in wavy slip. Fatigue tests on a 7075 aluminum alloy in vacuum have shown the underaged microstructure resulting in a higher threshold level and a greater FCG resistance, compared to the overaged one (reference 4). The difference is believed to be attributed to the following mechanism (references 4 and 15).

- Crystallographic transgranular crack growth and deflection occur in underaged alloys (typically in 7075-T351), containing shearable hardening Guinier-Preston (GP) zones of very small size (about 10 A diameter). Furthermore, Cu and Mg in solid solution lower the stacking fault energy and restrict cross-slip. In such a case, the damage process results from the to and fro motion of dislocations (very easy in the absence of dispersoid trapping points), which progressively induces dislocation jogging and cutting up. Therefore, a predominantly planar slip mode is observed leading to slow FCG.
- A smooth mode of crack growth occurs in overaged alloys, containing incoherent precipitates. The large precipitates (about 200 A) resist shearing and are widely spaced for the dislocations to pass between them. Furthermore, lesser contents of Cu and Mg in solid solution lead to easier cross-slip. Consequently, the FCG becomes greater with predominantly wavy slip mode and a flat crack path.

Besides the microstructure, stress ratio R has also been known to play a key role on FCG behavior of a metallic material. To account for the variation of FCG behavior with R, a self-consistent concept has been developed (references 16 through 23). The concept states that (a) two driving force parameters, stress intensity factor range (ΔK) and maximum stress intensity (K_{max}), are required to describe cyclic damage; (b) there are two thresholds corresponding to the parameters that must be satisfied for a crack to grow; (c) the two thresholds are intrinsic and are independent of specimen geometry; (d) a fundamental threshold curve can be developed that is independent of test methods defining the two thresholds from the asymptotic values; and (e) the two thresholds vary with the degree of slip planarity, microstructure, and environment. Based on this concept, the entire FCG behavior falls into five different classes (reference 21), defined by the experimental $\Delta K_{th} - R$ data, where ΔK_{th} is the threshold value of ΔK. This unified concept is applicable to a variety of materials at all crack growth rates (references 20 and 22) and short and long cracks (references 23 and 24).

This report discusses the role of aging-induced microstructure on the FCG behavior of a 7075 aluminum alloy in vacuum, using the two driving force parameters for threshold FCG, ΔK_{th} and K_{max}.

EXPERIMENTAL PROCEDURE

Two pieces of specimen material, a 7075 aluminum alloy, was received from Professor Stefanie Tschegg at the Institute of Meteorology and Physics, Vienna, Austria, via Dr. A. K. Vasudevan at the Office of Naval Research, Arlington, Virginia. The chemical composition is shown in table 1.

Table 1: Chemical Composition of Specimen Material (wt %)

Element	Measured	Nominal (Reference 25)
Cu	1.80	1.2 – 2.0
Mg	2.57	2.1 – 2.9
Mn	0.053	0.30
Si	0.126	0.50
Zn	5.65	5.1 – 6.1
Cr	0.02	0.18 – 0.40
Al	Balance	Balance

The measured Cr content, 0.02%, is less than the nominal one, 0.18 – 0.40%.

The two pieces of specimen material were initially subjected to the following heat treatments in air at the Institute of Meteorology and Physics, Vienna, Austria.

- Solution Treatment: Heating at 470°C for 45 min and Water Quenching
- Underaging Treatment of the 1st Piece: Freezing in Liquid Nitrogen for 15 min and Heating at 50°C for 10 min and at 117°C for 90 min
- Overaging T7351Treatment of the 2nd Piece: Heating at 107°C for 8 hr and at 163°C for 65 hr

From each of the underaged and overaged pieces, sheets of 24 x 4 x (0.18~0.23) mm were sliced with a diamond wheel saw. From each sheet, disks of 3 mm diameter were punched out with a circular sample punch. Subsequently, they were thinned electrolytically to foils of thickness 500 to 1000 A in a twin-jet electropolisher. The electrolyte was composed of 70% methyl alcohol and 30% nitric acid, chilled to –25°C. The foil was examined in a transmission electron microscope (TEM), JEOL JEM-100CX II, operating at an accelerating voltage of 120 kV.

The electrical conductivity was measured with a MAGNAFLUX FM-140 Digital Conductivity Meter. The hardness was determined using the Rockwell B (R_B) scale [1.6 mm (1/16 in.) ball indenter under a 100 kg load] in a Rockwell Hardness Tester.

The underaged and overaged pieces were machined to compact tension [C(T)] specimens, 24.1 mm (0.948 in.) wide and 4.6 mm thick (0.180 in.), in the T-L orientation, employing an Electrodischarge Machine, figure A-1.

For the fatigue testing, a closed-loop servo-hydraulic mechanical test machine (MTS) of 89 KN (20 kip) capacity was used. A vacuum system of 4 x 10^{-8} torr capacity was attached to the MTS machine. The MTS machine was suitably interfaced with a laboratory computer system for automated monitoring of FCG, using either compliance or d-c potential drop technique.

The FCG test was conducted under stress control in tension-tension cycling of frequency 10 Hz with a sinusoidal waveform and stress ratios, ranging from 0.1 to 0.85, at ambient temperature in vacuum of 4×10^{-8} torr. The fatigue crack length was continuously monitored with a laboratory computer system, using compliance technique. The fatigue loading procedure was K-decreasing (load shedding) for the FCG rate da/dN below 2.54 x 10^{-5} mm/cycle (1 x 10^{-6} in./cycle) and K-increasing for the da/dN above 2.54 x 10^{-5} mm/cycle (10^{-6} in./cycle).

After fatigue testing, the crack path profile, visible in the polished and etched side face of the specimen, was examined with an optical microscope. The crack surface morphology or fractograph was examined with a scanning electron microscope (SEM), JEOL JSM-5800LV, operating at an accelerating voltage of 20 kV.

RESULTS

FATIGUE CRACK GROWTH RATE AND STRESS INTENSITY RANGE

Raising R was observed to increase the FCG rate, da/dN, and reduce the ΔK_{th} under both underaged and overaged conditions. The typical variation of da/dN with ΔK is shown for underaged and overaged specimens at stress ratios R = 0.1 and 0.85 in figures A-2 and A-3. The FCG rates of underaged and overaged specimens are compared for R = 0.1 and 0.85 in figures A-4 and A-5. The da/dN is greater and the ΔK_{th} is smaller for the overaged condition than for the underaged one.

THRESHOLD STRESS INTENSITY RANGE AND MAXIMUM STRESS INTENSITY

The variations of ΔK_{th} and $K_{max} = \Delta K_{th}/(1- R)$, with R, are shown in figures A-6 and A-7, respectively. ΔK_{th} decreases with increasing R, steeply under the underaged condition and little under the overaged condition. The magnitude of ΔK_{th} at a given R is greater under the underaged condition than under the overaged condition. K_{max} increases with increasing R, gradually at R < 0.5 and steeply at R > 0.5. The magnitude of K_{max} at a given R is also greater under underaged condition than under overaged condition.

ΔK_{th} is plotted against K_{max} for the underaged and overaged conditions in figure A-8. Such a plot, called Fundamental Fatigue Threshold Curve, provides interrelation between the two parameters, ΔK_{th} and K_{max}, defining regions, where fatigue crack grows (above the curve) and where it does not (below the curve) (reference 21). In other words, the curve delineates a boundary where FCG

starts for a given K_{max} and indicates the resistance to threshold FCG. In figure A-8, the underaged curve is located above the overaged one. This demonstrates that the underaged treatment can offer a 7075 aluminum alloy a greater resistance to threshold FCG than the overaged one.

TRANSMISSION ELECTRON MICROSCOPE MICROGRAPH, ELECTRICAL CONDUCTIVITY, AND HARDNESS

The TEM, used for this investigation at the NAWCAD Patuxent River, Maryland (Code 4.3.4.2) laboratory, has a limited power of resolution and it cannot resolve tiny coherent precipitates of GP zone of 20 to 60 A diameter (reference 26). The TEM micrographs of the underaged and overaged pieces are shown in figures A-9 and A-10, respectively. That of the underaged one, figure A-9, shows a few precipitates, having diameter greater than 90 A, which appear to be semi-coherent transition precipitates η', dispersoids, and dislocations. Smaller and coherent GP zones are not visible. On the other hand, that of the overaged one, figure A-10, shows agglomerated incoherent precipitate-particles of η or $MgZn_2$ and some dispersoids.

The electrical conductivities and hardnesses of the underaged and overaged pieces are 27.6 and 40.1% International Annealed Copper Standard (IACS) and 89.3 and 77.5 R_B, respectively.

CRACK PATH

The typical crack paths in the underaged and overaged specimens are shown in figure A-11. In the underaged specimen, the fatigue crack path is transgranular, sharply-angled and tortuous, deflecting, and branching, figure A-11(a). Most of the deflections, including zigzagging, are observed to have occurred at grain boundaries and precipitate particles. Some of the deflection angles are measured to be about 30, 45, and 70 deg. On the other hand, in the overaged specimens, the fatigue crack path is transgranular and nearly straight linear with no deflection, figure A-11(b).

FATIGUE FRACTOGRAPH

A considerable difference is observable in fractographic features between the underaged and overaged conditions and between the stress ratios. The typical fractographs of the underaged and overaged specimens of stress ratios R = 0.1 and R = 0.85 are shown for two different FCG rates, (7.6~12.7) x 10^{-10} m/cycle and (1.0~1.5) x 10^{-10} m/cycle [(3~5) x 10^{-8} in./cycle and (4~6) x 10^{-9} in./cycle] in figures A-12 and A-13, respectively. The underaged condition is characterized by a faceted FCG. The facets are formed on crystallographic planes, their orientation changes from grain to grain, and the crack surface is quite rough. The crystallographic facets are sharper and cover a more area at R = 0.85 than at R = 0.1. They are consistent with a predominantly planar slip mode, which preferentially occurs when the precipitates are shearable. On the other hand, the crack surface of the overaged specimen is relatively flat, exhibiting some featureless regions, patches of faint striations, and dimples. Better defined and more dimples are observable at R = 0.85 than at R = 0.1.

DISCUSSION

FATIGUE CRACK GROWTH BEHAVIOR

The observed increasing da/dN and decreasing ΔK_{th} with increasing R in the underaged and overaged 7075 aluminum alloy, figures A-2 and A-3, are in agreement with the results obtained for the other materials (references 2, 8, 9, 12, 21, and 27 through 43). The observed greater da/dN and smaller ΔK_{th} under the overaged condition than under the underaged condition in vacuum, figures A-4 and A-5, are also reported by other investigators (references 2, 4, 9, and 44).

ΔK_{th} decreased and K_{max} increased with increasing R from 0.1 to 0.85, figures A-6 and A-7. The rate of ΔK_{th} decrease with increasing R is greater in the underaged condition than in the overaged condition. Such a decreasing ΔK with increasing R was also observed during the study on AerMet 100 steel (reference 45) and 2618-T651 aluminum alloy (reference 46) in vacuum. On the other hand, some investigators reported independence of ΔK_{th} on R in vacuum (references 2, 4, 9, 44, and 47). Throughout the range of R employed, ΔK_{th} and K_{max} are greater, evidencing a greater resistance to the threshold FCG, in the underaged condition than in the overaged condition. This is confirmed by the two Fundamental Fatigue Threshold Curves, one for the underaged condition located above the other for the overaged condition, figure A-8.

SPECIMEN MATERIAL 7075 ALUMINUM ALLOY

7075 aluminum alloy contains three types of second-phase particles; namely, secondary intermetallics, dispersoids, and metastable precipitates, which influence mechanical properties, including fatigue resistance (reference 3).

Secondary intermetallics (~1 to 30 μm) are the largest of these particles. They form during solidification, combining impurity elements Fe and Si with Al and solute atoms. These coarse intermetallic particles do not contribute to strength. However, as they are brittle, they fracture or separate from the matrix at high local strains. Decreasing volume fraction of these particles increases fracture toughness and FCG resistance at high ΔK.

Dispersoid particles (0.02 to 0.3 μm) form by solid-state precipitation of Cr and Zr at temperatures above about 425°C. Under monotonic tension loading, dispersoids decrease energy to propagate cracks by initiating microvoids that coalesce to link incipient cracks initiated at larger constituents particles. Energy required to propagate a crack under monotonic tension loading increases as volume fraction decreases and as dispersoid spacing decreases. Dispersoids do not affect the FCG resistance at intermediate ΔK.

Metastable precipitates (0.002 to 0.01 μm) are the smallest type second-phase particles, and they contain the major solute elements Zn, Mg, and Cu. Precipitates develop in uncontrolled manner during quenching or in a controlled manner during aging. The structure and composition of precipitates have a direct effect on strength and resistance to environment.

Considering the temperatures (50°C to 163°C), employed for the underaging and overaging treatments, the characteristics (kind, size, and spacing) of the aging-produced precipitates must be the deciding factors for the different FCG behaviors observed.

Quenching an aluminum alloy after a solution heat treatment generally results in a low electrical conductivity, because a large part of the constituents present are retained in solid solution (reference 48). The electrical conductivity decreases in the initial stage of the subsequent aging due to GP zone and increases in the later stage (particularly at elevated temperatures) due to removal of constituents from solid solution (reference 48). On the one hand, the hardness is decreased by aging. The measured electrical conductivity for underaging, 27.6% IACS, is lower than that for peak aging of 7075 aluminum alloy (7075-T6), 30.5~36.0% IACS (reference 49). The measured one for overaging, 40.1% IACS, is in agreement with that for 7075-T73 aluminum alloy, 40.0~43.0% IACS (reference 49). The measured hardness for underaging, 89.3 R_B, is greater than that for 7075-T6 aluminum alloy, 84.0 R_B, and the one for overaging, 77.5 R_B, is close to that for 7075-T73 aluminum alloy, 78.0 R_B (reference 49).

FATIGUE CRACK GROWTH MECHANISMS

Though the coherent precipitates were not clearly resolved, as figure A-9 shows, it is believed that the underaging must have produced coherent precipitates (reference 48). On the other hand, the overaging produced incoherent precipitates of $MgZn_2$, as shown in figure A-10. The crack path in the underaged specimen is tortuous, deflecting, and branching,.figure A-11(a), whereas that in the overaged specimen is nearly straight linear without deflecting or branching, figure A-11(b). The fractographic features are crystallographic facets in the underaged specimen and relatively flat plateaus, some with faint striations, in the overaged specimen, figures A-12 and A-13. These different characteristics of microstructure, crack path, and fractograph must be associated with the aforementioned different FCG behaviors/resistances of the underaged and overaged specimens.

The coherent particles are known to be sheared by dislocations and promote planar slip. Therefore, the microstructure of the underaged specimen, hardened by coherent particles, gives rise to inhomogeneous dislocation distribution upon plastic deformation, leading to the formation of pile-up ahead of crack tip. During the unloading part of the fatigue cycle, the back stress within the pile-up forces the dislocations to move in the opposite direction on the same slip plane, because the particles are already destroyed in this plane. This reversed dislocation movement/slip will continue until the back stress equals the friction stress of the particle free matrix. Consequently, the reversible slip increases the number of fatigue cycles necessary to produce unit crack extension or slows the FCG (references 4, 13, 15, and 50). and raises the threshold level. Besides, Cu and Mg in solid solution lower the stacking fault energy and restrict cross-slip, leading to planar slip (references 51 and 52). The planar slip favors cracking along slip facets and occurrence of crack deflection and branching. The effective stress intensity factor or the driving force for FCG for a deflected and branched crack is considerably smaller than that of a straight crack of the same (projected) length, resulting in slower FCG and higher threshold level (references 53 through 57).

Overaging produces precipitates incoherent with the matrix. The incoherent precipitates are nonshearable, widely spaced for the dislocations to pass between them, and looped and bypassed by dislocations, favoring cross-slip. In addition, the dislocation movement during unloading part of the fatigue cycle is irreversible and hence the crack tip damage per cycle is much higher, as well as the FCG rate, than for the underaged condition. This results in wavy slip, which promotes more homogeneous deformation, reduces crack tortuosity, and induces poor fatigue resistance. This wavy slip mode and the accumulation of dislocations combined with the precipitates cause dimple formation and flat crack growth. Furthermore, lesser contents of Cu and Mg in solid solution lead to easier cross-slip, greater FCG (reference 52), and lower threshold level.

CONCLUSIONS

- The underaging induced greater resistance to threshold FCG, evidenced by greater ΔK_{th} and K_{max}, than the overaging.

- The underaging resulted in a microstructure containing coherent shearable precipitates and a faceted tortuous crack path, whereas the overaging resulted in a microstructure containing incoherent nonshearable precipitates and a nearly straight crack path.

- The greater threshold FCG resistance of the underaged specimen is attributed to the coherent shearable precipitates. Those precipitates facilitate reversible planar slip, promote crack deflection and branching, lower the effective stress intensity factor for FCG, and slow down FCG.

REFERENCES

1. Verkin, B. I.: "The Effect of Vacuum on the Fatigue Behavior of Metals and Alloys," Materials Science and Engineering, 1979, Vol. 41, p. 149.

2. Kirby, B. R. and Beevers, C. J.: "Slow Fatigue Crack Growth and Threshold Behaviour in Air and Vacuum of Commercial Aluminum Alloys," Fatigue of Engineering Materials and Structures, 1979, Vol. 1, pp. 203-215.

3. Bucci, R. J., Thakker, A. B., Sanders, T. H., Sawtell, R. R., and Staley, J. T.: "Ranking 7XXX Aluminum Alloy Fatigue Crack Growth Resistance Under Constant Amplitude and Spectrum Loading," in *Effect of Load Spectrum Variables on Fatigue Crack Initiation and Propagation*, ASTM STP 714, D. F. Bryan and J. M. Potter, eds., American Society for Testing and Materials, 1980, pp. 41-78.

4. Petit, J., Renaud, P., and Violan, P.: "Effect of Microstructure on Crack Growth in a High Strength Aluminum Alloys," Proceedings of the 4th European Conference on Fracture, Leoben, Austria, K. L. Maurer, F. E. Matzer, eds., EMAS, Warley, U. K., 1982, Vol. 2, pp. 426-433.

5. Forsyth, P. J.E. and Bowen, A. W.: "The Relationship between Fatigue Crack Behaviour and Microstructure in 7178 Aluminum Alloy," Int. J. Fatigue, 1981, Vol. 2, pp. 17-25.

6. Renaud, P., Violan, P., Petit, J., and Ferton, D.: "Microstructural Influence on Fatigue Crack Growth Near Threshold in 7075 Alloy," Scripta Met., 1982, Vol. 16, pp. 1311-1316.

7. McKittrick, J., Liaw, P. K., Kwun, S. I., and Fine, M. E.: "Threshold for Fatigue Macrocrack Propagation in Some Aluminum Alloys," Met. Trans. A, 1981, Vol. 12A, pp. 1535-1539.

8. Yoder, G. R., Colley, L. A., and Crooker, T. W.: "On Microstructural Control of Near Threshold Fatigue Crack Growth in 7000 Series Aluminum Alloys," Scripta Met., 1982, Vol. 16, pp. 1021-1025.

9. Lafarie-Frenot, M. and Gasc, C.: "The Influence of Age-Hardening on Fatigue Crack Propagation Behaviour in 7075 Aluminum Alloy in Vacuum," Fatigue of Engineering Materials and Structures, 1983, Vol. 6, pp. 329-344.

10. Carter, R. D., Lee, E. W., Starke, E. A., Jr., and Beevers, C. J.: "The Effect of Microstructure and Environment on Fatigue Crack Closure of 7475 Aluminum Alloy," Met. Trans. A, 1984, Vol. 15A, pp. 555-563.

11. Irving, P. E. and McCartney, L. N.: "Prediction of Fatigue Crack Growth Rates: Theory, Mechanisms, and Experimental Results," Metal Science., 1977, Vol. 11, pp. 351-361.

12. Vasudevan, A. K. and Bretz, P. E.: "Near-Threshold Fatigue Crack Growth Behavior of 7XXX and 2XXX Alloys: A Brief Review" in *Fatigue Crack Growth Threshold Concepts*, Davidson D. L. and Suresh, S. eds., The Metallurgical Society of AIME, 1983, pp. 25-42.

13. Lindigkeit, J., Terlinde, G., Gysler, A., and Lutjering, G.: "The Effect of Grain Size on the Fatigue Crack Propagation Behavior of Age-Hardened Alloys in Inert and Corrosive Environment," Acta Met., 1979, Vol. 27, pp.1717-1726.

14. Lindigkeit, J., Gysler, A., and Lutjering, G.: "The Effect of Microstructure on the Fatigue Crack Propagation Behavior of an Al-Zr-Mg-Cu Alloy," Met. Trans., 1981, Vol. 12A, pp. 1613-1619.

15. Blankenship, C. P., Jr. and Starke, E. A., Jr.: "The Fatigue Crack Growth Behaviour of the Al-Cu-Li Alloy Weldlite 49," Fatigue of Engineering Materials and Structures, 1991, Vol. 14, pp. 103-114.

16. Vasudevan, A. K., Sadananda, K., and Louat, N.: "Two Critical Stress Intensities for Threshold Fatigue Crack Propagation," Scripta Metallurgica et Materialia, 1993, Vol. 28, pp. 65-70.

17. Vasudevan, A. K., Sadananda, K., and Louat, N.: "A Review of Crack Closure, Fatigue Crack Threshold and Related Phenomena," Materials Science and Engineering, 1994, Vol. A188, pp. 1-22.

18. Louat, N., Sadananda, K., Duesbery, M. S., and Vasudevan, A. K.: "A Theoretical Evaluation of Crack Closure," Met. Trans. A, 1993, Vol. 24A, pp. 2225-2232.

19. Sadananda, K. and Vasudevan, A. K.: "Analysis of Fatigue Crack Closure and Thresholds," in *Fracture Mechanics,* 25th Volume, ASTM STP 1220, F. Erdogan, ed., American Society for Testing and Materials, 1995, pp. 484-500.

20. Vasudevan, A. K. and Sadananda, K.: "Fatigue Crack Growth Behavior of Composites," Metallurgical and Material Transactions, 1995, Vol. 26A, pp. 3199-3210.

21. Vasudevan, A. K. and Sadananda, K.: "Classification of Fatigue Crack Growth Behavior," Metallurgical and Materials Transactions A, 1995, Vol. 26A, pp. 1221-1234.

22. Sadananda, K. and Vasudevan, A. K.: "Fatigue Crack Growth Behaviour in Titanium Aluminides," Materials Science and Engineering, 1995, Vol. A192/193, pp. 490-501.

23. Sadananda, K. and Vasudevan, A. K.: "Short Crack Growth Behavior," in *Fatigue and Fracture Mechanics,* 27th Volume, ASTM STP 1296, R. S. Piascik, J. C. Newman, and N. E. Dowling, eds., American Society for Testing and Materials, 1997, pp. 301-316.

24. Sadananda, K. and Vasudevan, A. K.: "Short Crack Growth and Internal Stress," International Journal of Fatigue, 1997, Vol. 19, pp. S99-S108.

25. Brown, W. F., Mindlin, H., and Ho, C. Y.: *Aerospace Structural Metals Handbook*, CINDAS/USAF CRDA Handbooks Operation, Purdue University, 1995, Vol. 3, Code 3207.

26. Thomas, G.: *Transmission Electron Microscopy of Metals*, John Wiley & Sons, Inc., 1962, p. 237.

27. Schmidt, R. A. and Paris, P. C.: "Threshold for Fatigue Crack Propagation and the Effects of Load Ratio and Frequency," in *Progress in Flaw Growth and Fracture Toughness Testing,* ASTM STP 536, American Society for Testing and Materials, Philadelphia, PA, 1973, pp. 79-94.

28. Ritchie, R. O., Suresh, S., and Moss, C. M.: "Near-Threshold Fatigue Crack Growth in 2 ¼ Cr – 1Mo Pressure Vessel Steel in Air and Hydrogen," Journal of Engineering Materials and Technology, ASME Trans., 1980, Vol. 102, pp. 293-299.

29. Stewart, A. T.: "The Influence of Environment and Stress Ratio on Fatigue Crack Growth at Near-Threshold Stress Intensities in Low-Alloy Steels," Engineering Fracture Mechanics, 1980. Vol. 13, pp. 463-478.

30. Suresh, S., Zaminski, G. F., and Ritchie, R. O.: "Oxide-Induced Crack Closure: An Explanation for Near-Threshold Corrosion Fatigue Crack Growth Behavior," Metall. Trans. A, 1981, Vol. 12A, pp. 1435-1443.

31. Nakai, Y., Tanaka, K., and Nakanishi, T.: "The Effects of Stress Ratio and Grain Size on Near-Threshold Fatigue Crack Propagation in Low-Carbon Steel," Engineering Fracture Mechanics, 1981, Vol. 15, pp. 291-302.

32. Blom, A. F.: "Near-Threshold Fatigue Crack Growth and Crack Closure in 17-4 PH Steel and 2024-T3 Aluminum Alloy," in *Fatigue Crack Growth Threshold Concepts,* D. L. Davidson and S. Suresh, eds., The Metallurgical Society of AIME, 1984, pp. 263-279.

33. Gray, G. T. III, William, J. C., and Thompson, A. W.: "Roughness-Induced Crack Closure: An Explanation for Microstructurally Sensitive Fatigue Crack Growth," Met.Trans. A, 1983, Vol. 14A, pp. 421-433.

34. Liaw, P. T., Saxena, A., Swaminathan, V. P., and Shih, T. T.: "Influence of Temperature and Load Ratio on Near-Threshold Fatigue Crack Growth Behavior of CrMoV Steel," in *Fatigue Crack Growth Threshold Concepts,* D. L. Davidson and S. Suresh, eds., The Metallurgical Society of AIME, 1984, pp. 205-223.

35. Liaw, P. K., Leax, T. R., and Donald, J. K.: "Fatigue Crack Growth Behavior of 4340 Steels," Acta Metall., 1987, Vol. 35, pp. 1415-1432.

36. Cadman, A. J., Nicholson, C. E., and Brook, R.: "Influence of R Ratio and Orientation on the Fatigue Crack Threshold ΔK_{th}, and Subsequent Crack Growth of a Low-Alloy Steel," in *Fatigue Crack Growth Threshold Concepts,* D. L. Donaldson and S. Suresh, eds., The Metallurgical Society of AIME, 1984, pp. 281-298.

37. Esaklul, K. A., Wright, A. G., and Gerberich, W. W.: "An Assessment of Internal Hydrogen Versus Closure Effects on Near-Threshold Fatigue Crack Propagation," in *Fatigue Crack Growth Threshold Concepts,* D. L. Davidson and S. Suresh, eds., The Metallurgical Society of AIME, 1984, pp. 299-326.

38. Ritchie, R. O: "Near-Threshold Fatigue Crack Propagation in Ultra-High Strength Steel: Influence of Load Ratio and Cyclic Strength," Journal of Engineering Materials and Technology, Transactions of ASME, 1977, Vol. 99, pp. 195-204.

39. Ritchie, R. O.: "Near-Threshold Fatigue-Crack Propagation in Steels," International Metals Reviews, 1979, Nos. 5 and 6, pp. 205-230.

40. Doker, H. and Marci, G.: "Threshold Range and Opening Stress Intensity Factor in Fatigue," International Journal of Fatigue, 1983, Vol. 5, pp. 187-191.

41. Suresh, S., Vasudevan, A. K., and Bretz, P. E.: "Mechanisms of Slow Fatigue Crack Growth in High Strength Aluminum Alloys: Role of Microstructure and Environment," Metall. Trans. A, 1984, Vol. 15A, pp. 369-379.

42. Han, L. X. and Suresh, S.: "High-Temperature Failure of an Alumina-Silicon Carbide Composite under Cyclic Loads: Mechanisms of Fatigue Crack Tip Damage," Journal of American Ceramic Society, 1989, Vol. 72, pp. 1233-1238.

43. Vasudevan, A. K. and Sadananda, K.: "Fatigue Crack Growth in Metal Matrix Composites," Scripta Metallurgica et Materialia, 1993. Vol. 28, pp. 837-842.

44. Doker, H. and Peters, M.: "Fatigue Threshold Dependence on Material, Environment and Microstructure", in *Fatigue* '84, Proceedings of 2nd International Conference on Fatigue and Fatigue Thresholds, C. J. Beevers, ed., Engineering Materials Advisory Services, Warley, United Kingdom, 1984, p. 275.

45. Lee, E. U.: Unpublished Work.

46. Petit, J. and Maillard, J. L.: "Environment and Load Ratio Effects on Fatigue Crack Propagation Near Threshold Conditions," Scripta Met., 1980, Vol. 14, pp. 163-166.

47. Cooke, R. J., Irving, P. E., Booth, G. S., and Beevers, C. J.: "The Slow Fatigue Crack Growth and Threshold Behaviour of a Medium Carbon Alloy Steel in Air and Vacuum," Engineering Fracture Mechanics, 1975, Vol. 7, pp. 69-77.

48. Hatch, J. E.: *Aluminum: Properties and Physical Metallurgy*, American Society for Metals, Metals Park, OH, 1984, pp. 145-148.

49. Aerospace Materials Specification, AMD-2658, "Hardness and Conductivity Inspection of Wrought Aluminum Alloy Parts," Society of Automotive Engineers, Warrendale, PA, 1999.

50. Hornbogen, E. and Zum Gahr, K. H.: "Microstructure and Fatigue Crack Growth in a γ-Fe-Ni-Al Alloy," Acta Met., 1976, Vol. 24, pp. 581-592.

51. Tomkins, B.: "Role of Mechanics in Corrosion Fatigue," Metal Science, 1979, Vol. 13, pp. 387-395.

52. Selines, R. J.: "The Fatigue Behavior of High Strength Aluminum Alloys," Doctor of Science Thesis, MIT, 1971.

53. Lin, F. S. and Starke, E. A., Jr.: "The Effect of Copper Content and Degree of Recrystallization on the Fatigue Resistance of 7XXX-Type Aluminum Alloys – Part II. Fatigue Crack Propagation," Mater. Sci. Engng., 1980, Vol. 43, pp. 65-76.

54. Suresh, S.: "Crack Deflection: Implications for the Growth of Long and Short Fatigue Cracks," Met. Trans. A, 1983, Vol. 14A, pp. 2375-2385.

55. Suresh, S.: "Micromechanisms of Fatigue Crack Growth Retardation Following Overloads," Engr. Frac. Mech., 1983, Vol. 18, pp. 577-593.

56. Suresh, S.: "Fatigue Crack Deflection and Fracture Surface Contact: Micromechanical Models," Met. Trans. A, 1985, Vol. 16A, pp. 249-260.

57. Suresh, S.: *Fatigue of Materials*, Cambridge University Press, 1991, pp. 182-189.

APPENDIX A
FIGURES

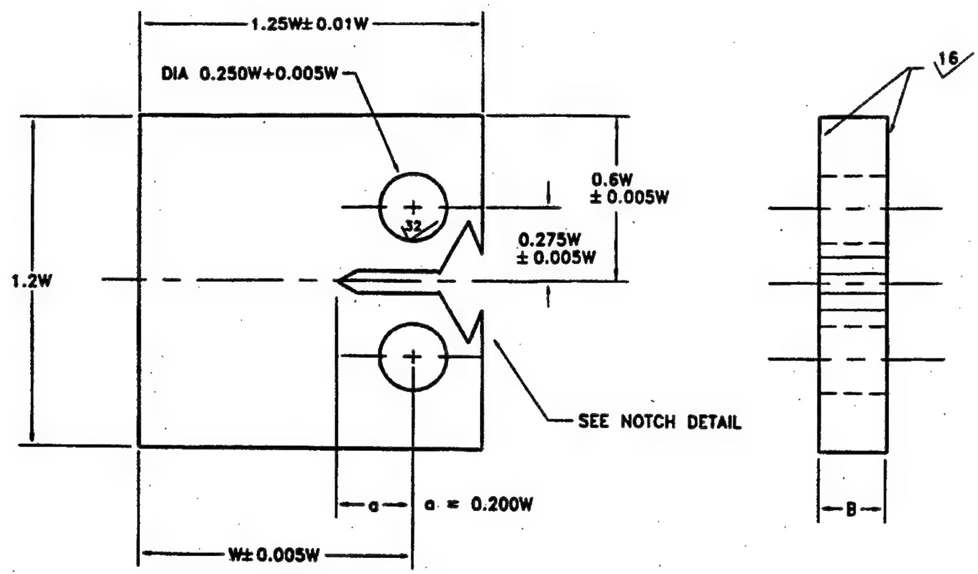

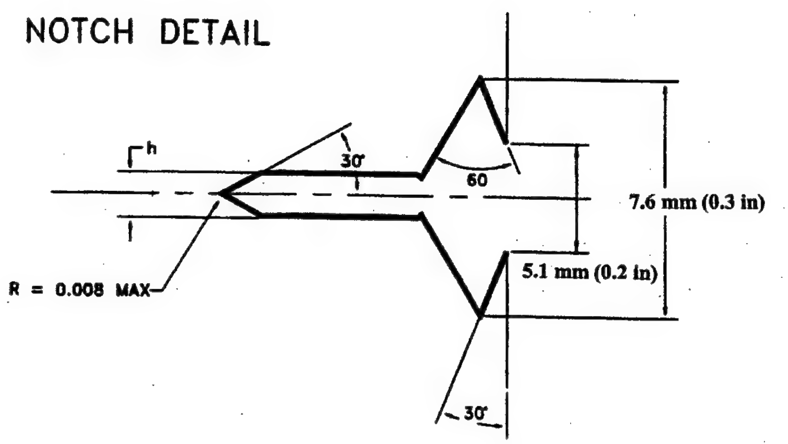

W = 24.1 mm (0.95 in)
B = 4.6 mm (0.18 in)
H = 1.6 mm (1/16 in)

Figure A-1: C(T) Specimen for FCG Testing

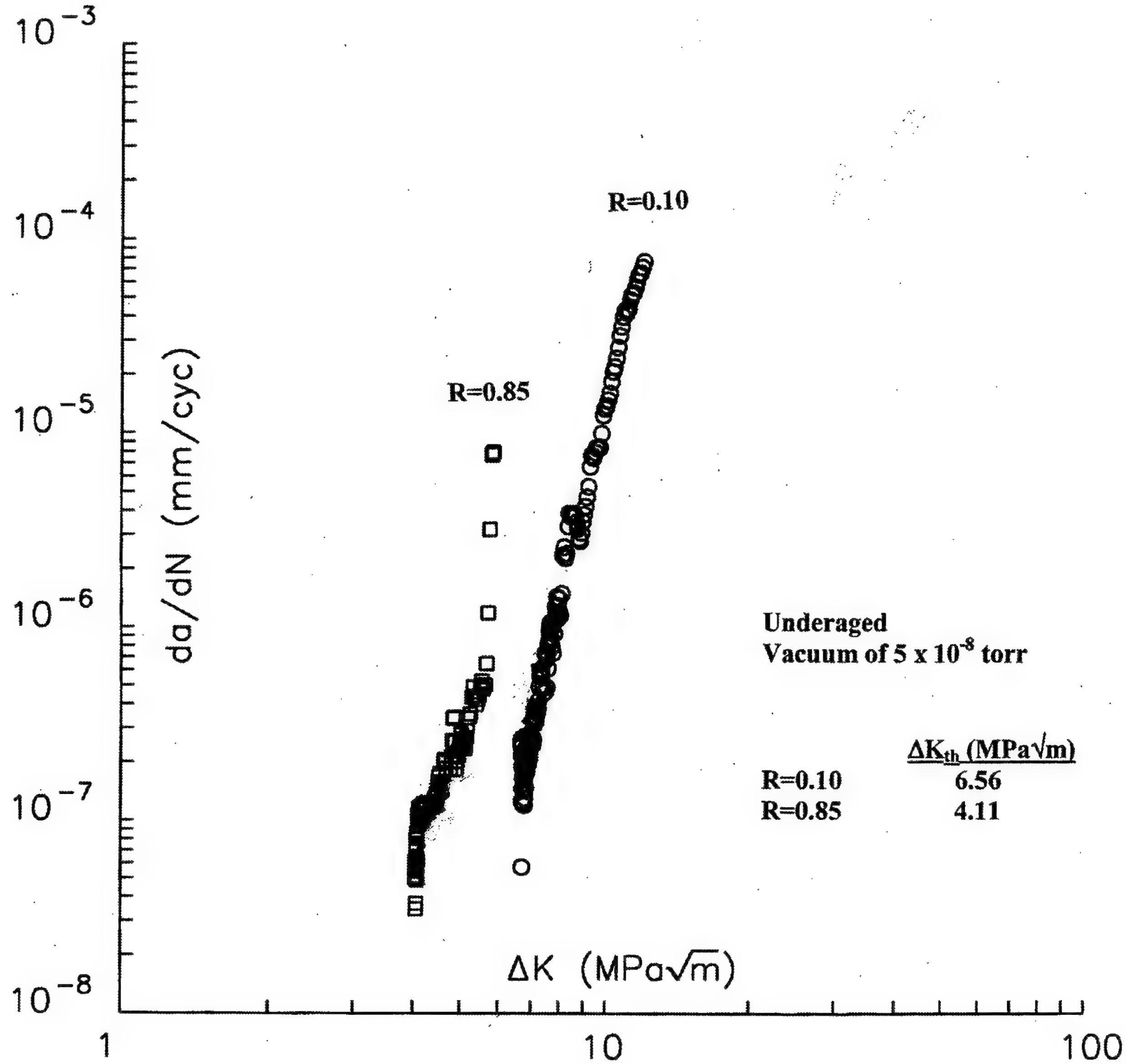

Figure A-2: Variation of FCG Rate, da/dN, with ΔK in Underaged Specimens at Stress Ratios, R, 0.10 and 0.85

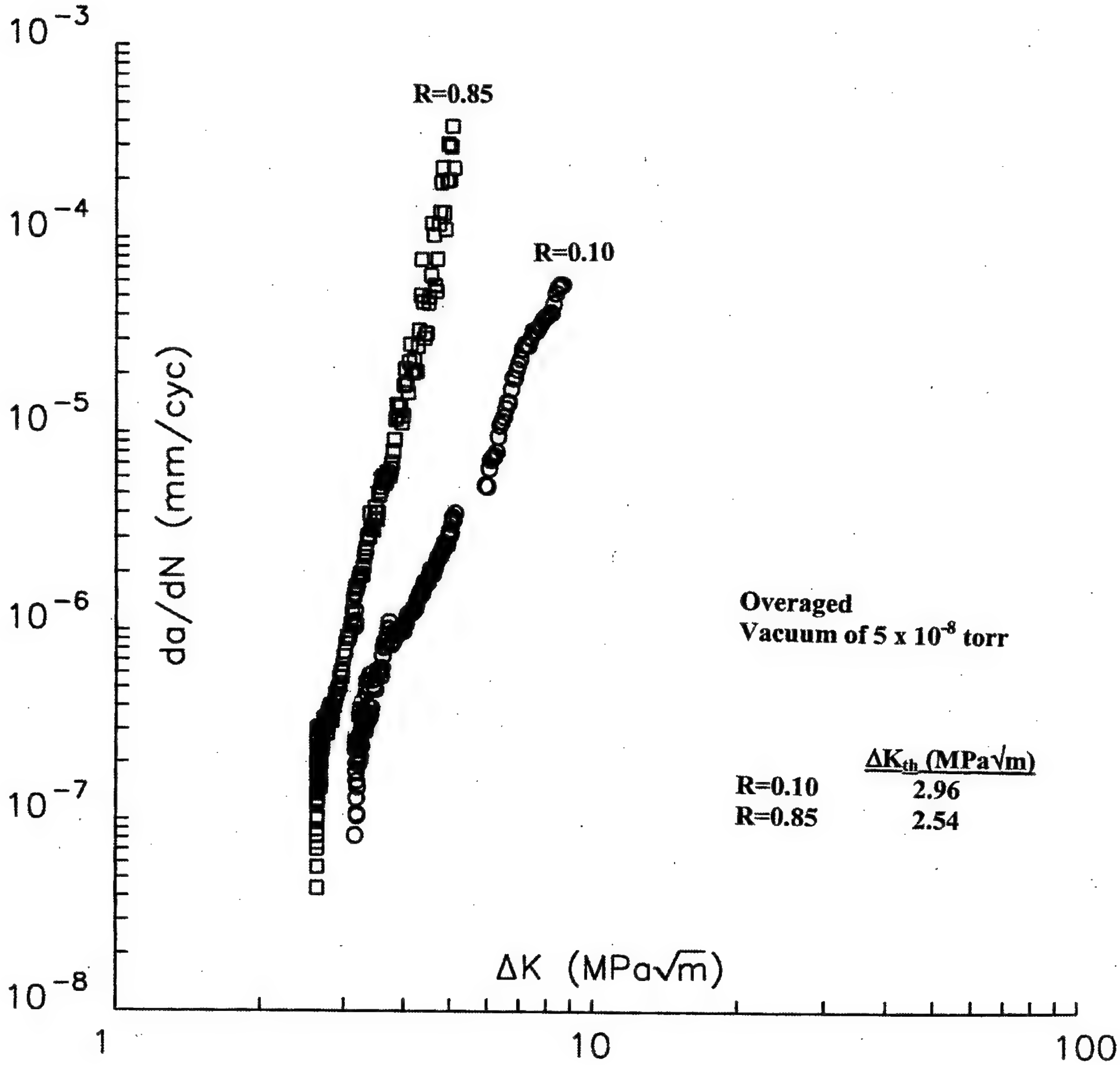

Figure A-3: Variation of FCG Rate, da/dN, with ΔK in Overaged Specimens at Stress Ratios, R, 0.10 and 0.85

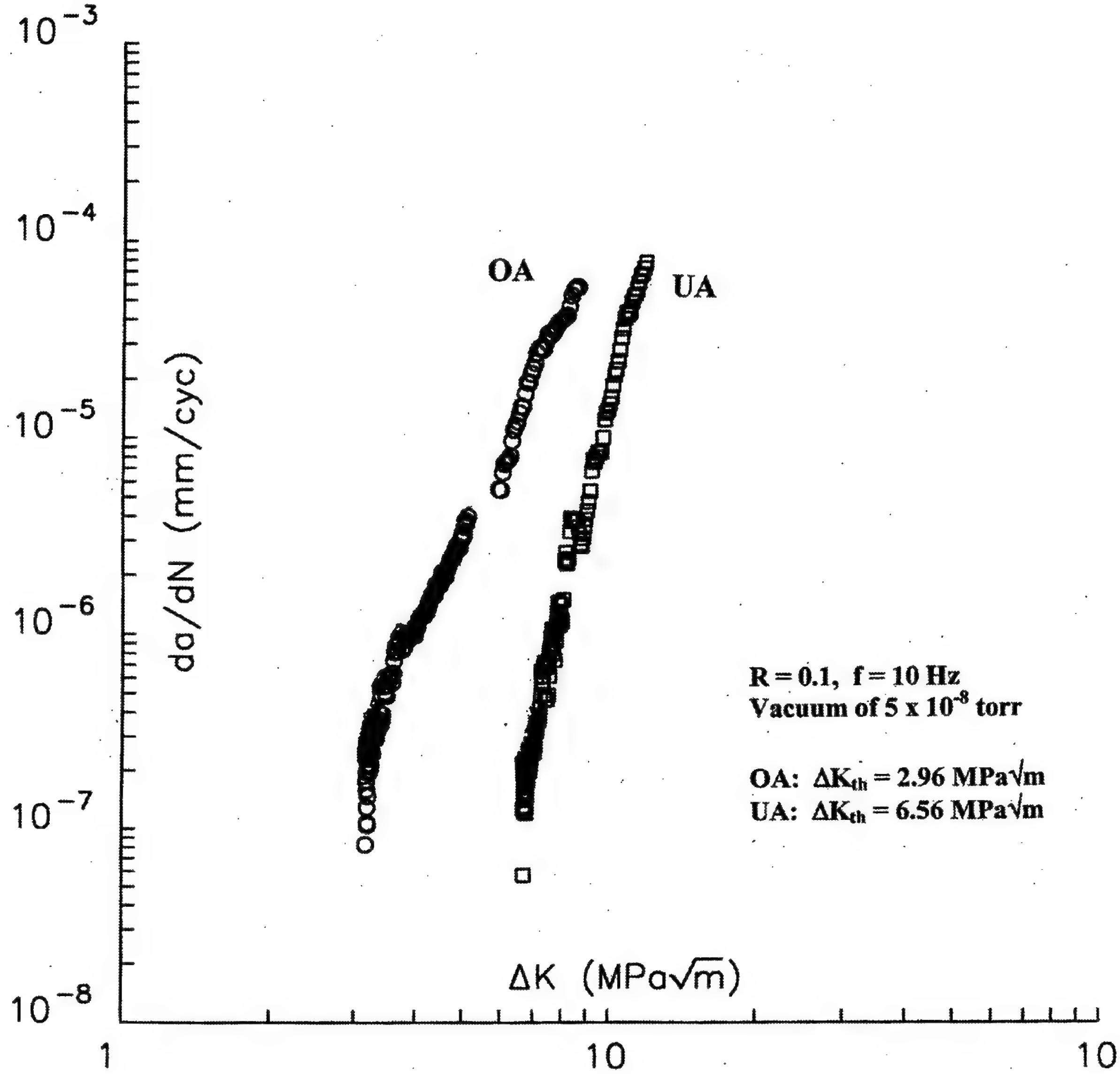

Figure A-4: Variation of FCG Rate, da/dN, with ΔK in Underaged and Overaged Specimens at Stress Ratio, R, 0.10

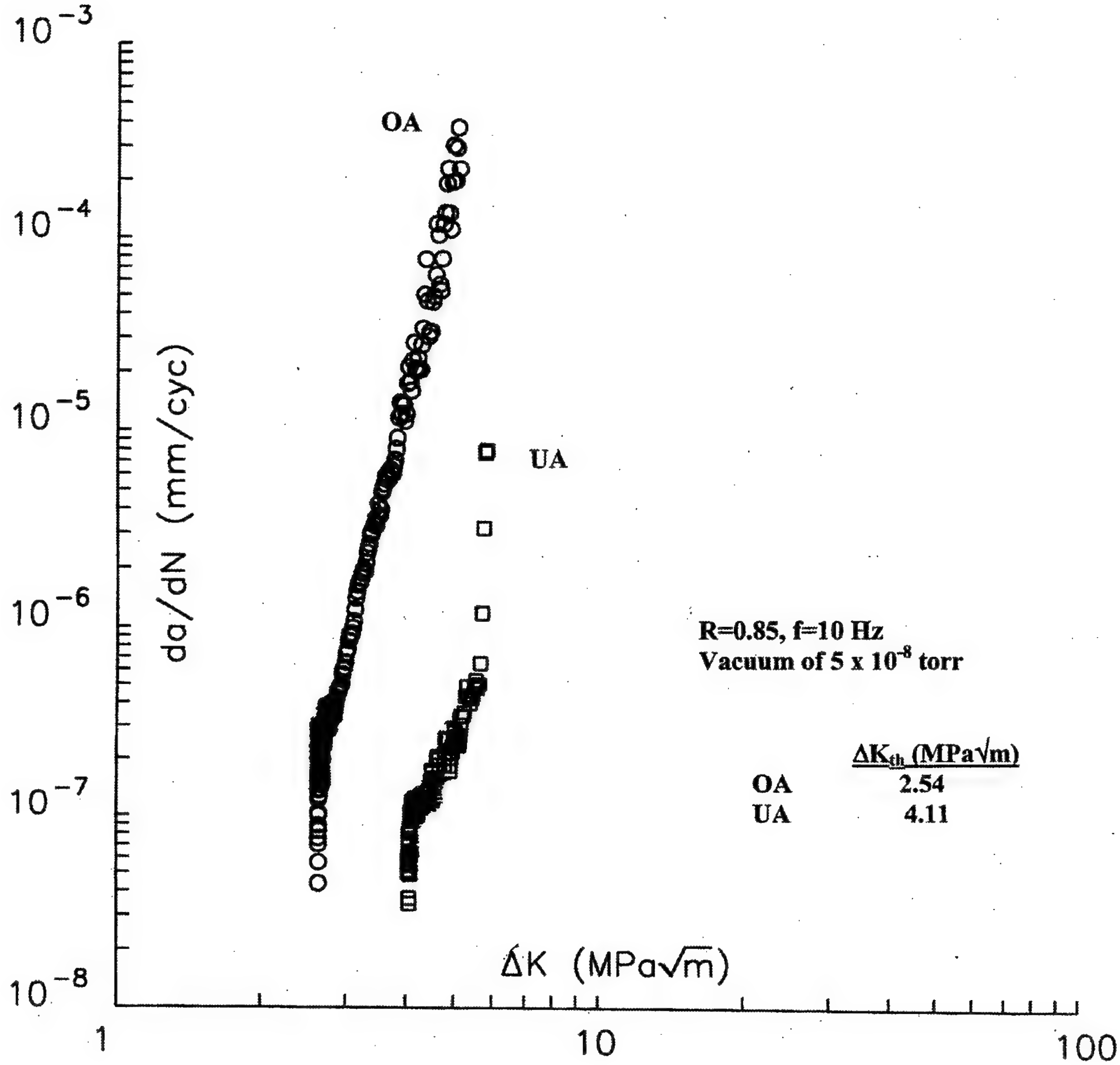

Figure A-5: Variation of FCG Rate, da/dN, with ΔK in Underaged and Overaged Specimens at Stress Ratio, R, 0.85

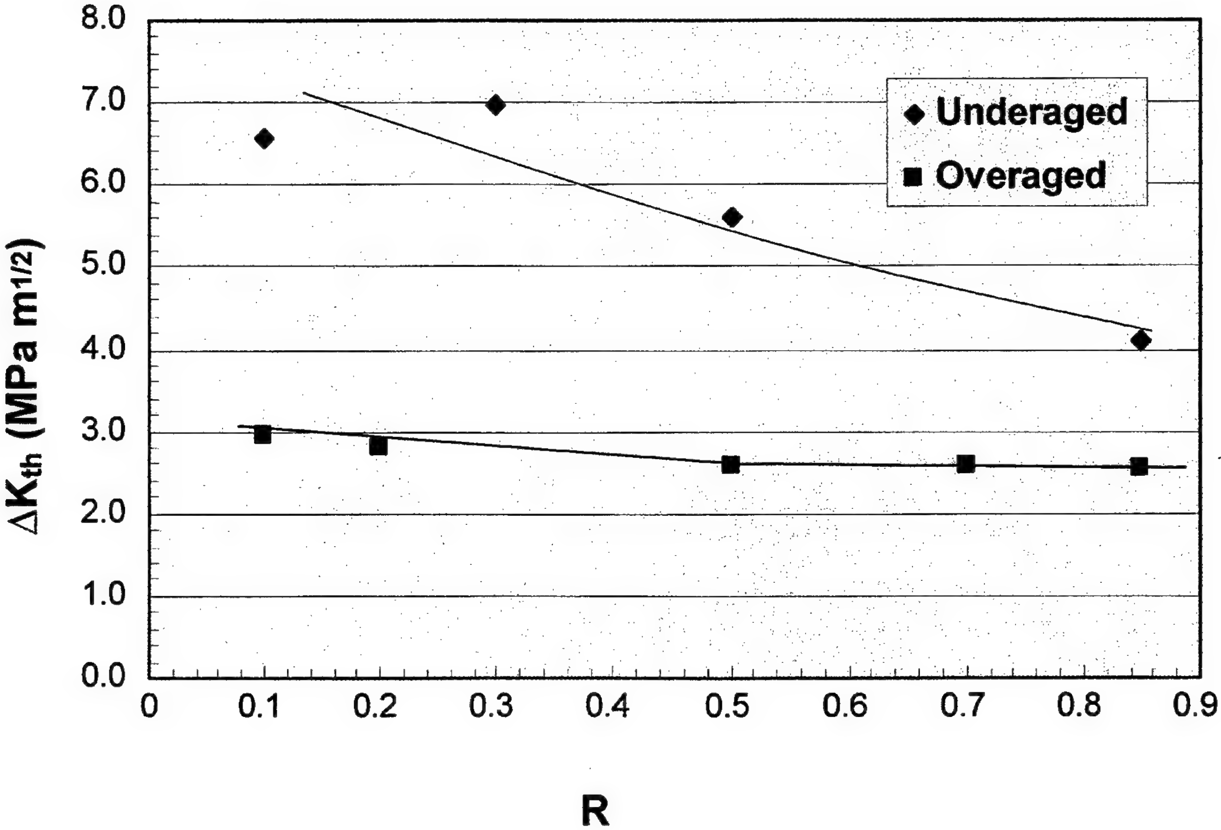

Figure A-6: Variation of ΔK_{th} with Stress Ratio, R, in Underaged and Overaged Specimens

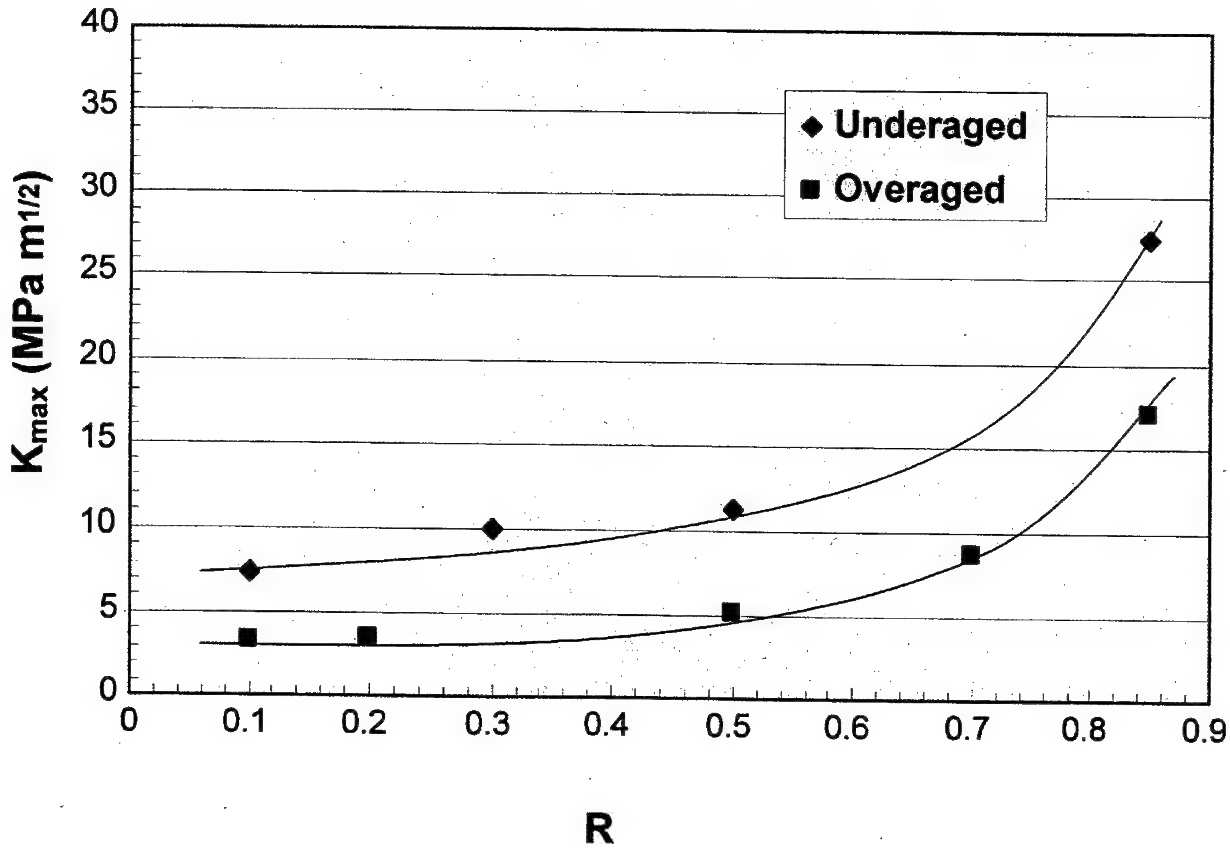

Figure A-7: Variation of K_{max} with Stress Ratio, R, in Underaged and Overaged Specimens

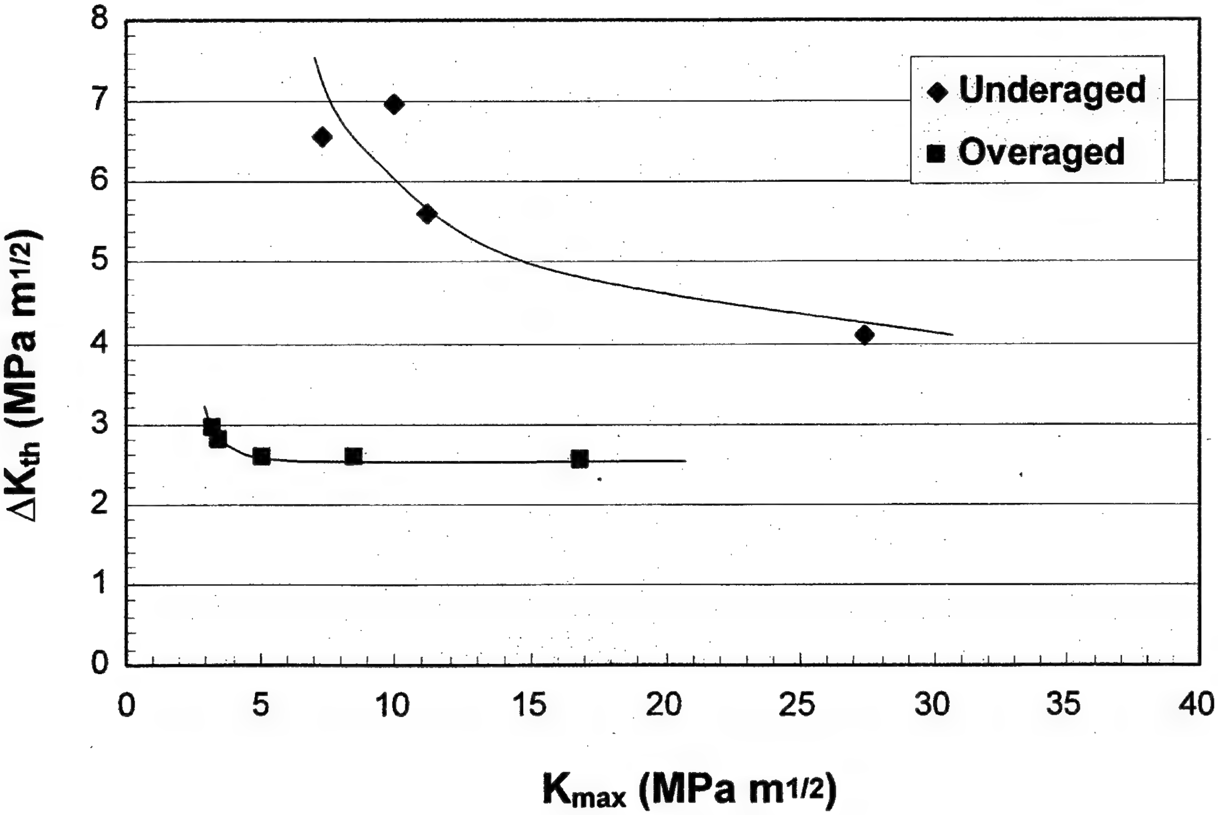

Figure A-8: Variation of ΔK_{th} with K_{max} (Fundamental Threshold Curves) for Underaged and Overaged Specimens

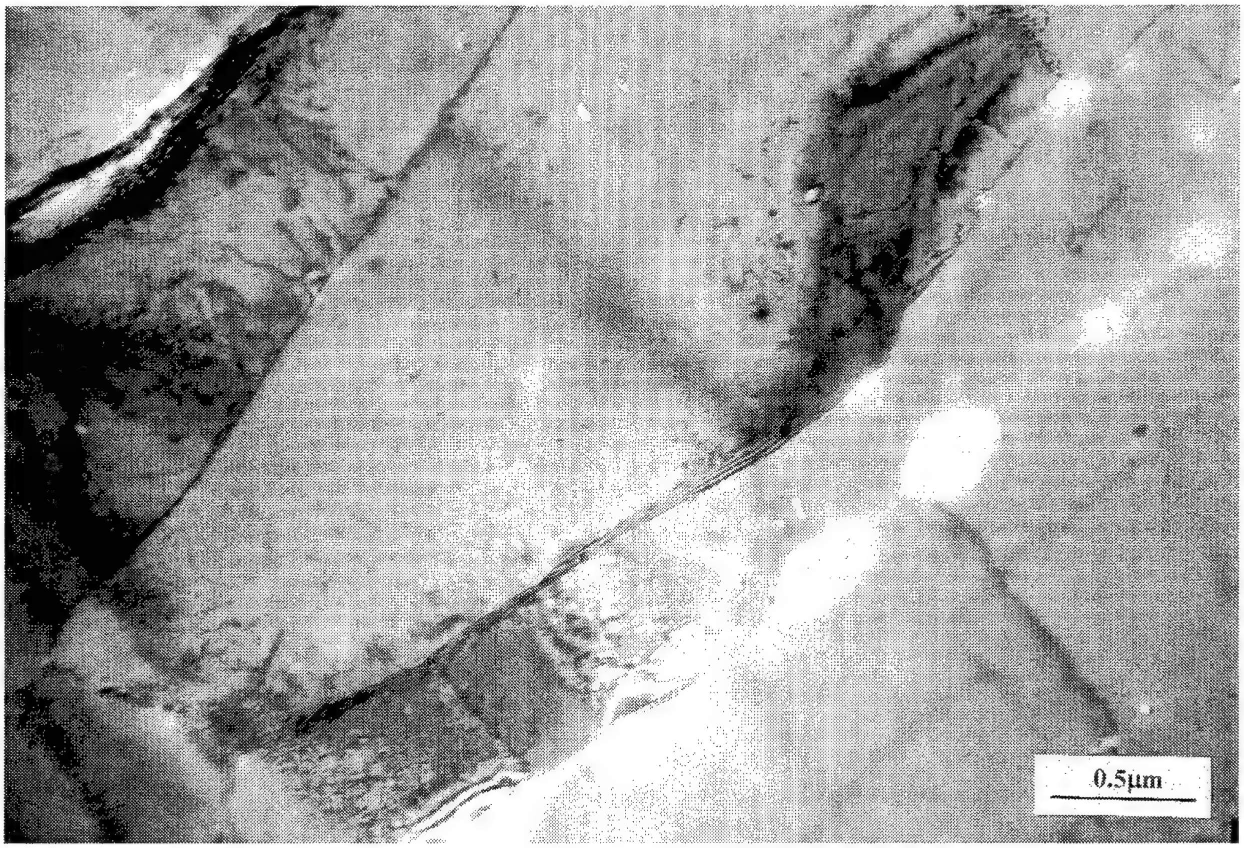

Figure A-9: TEM Micrograph of Underaged Specimen

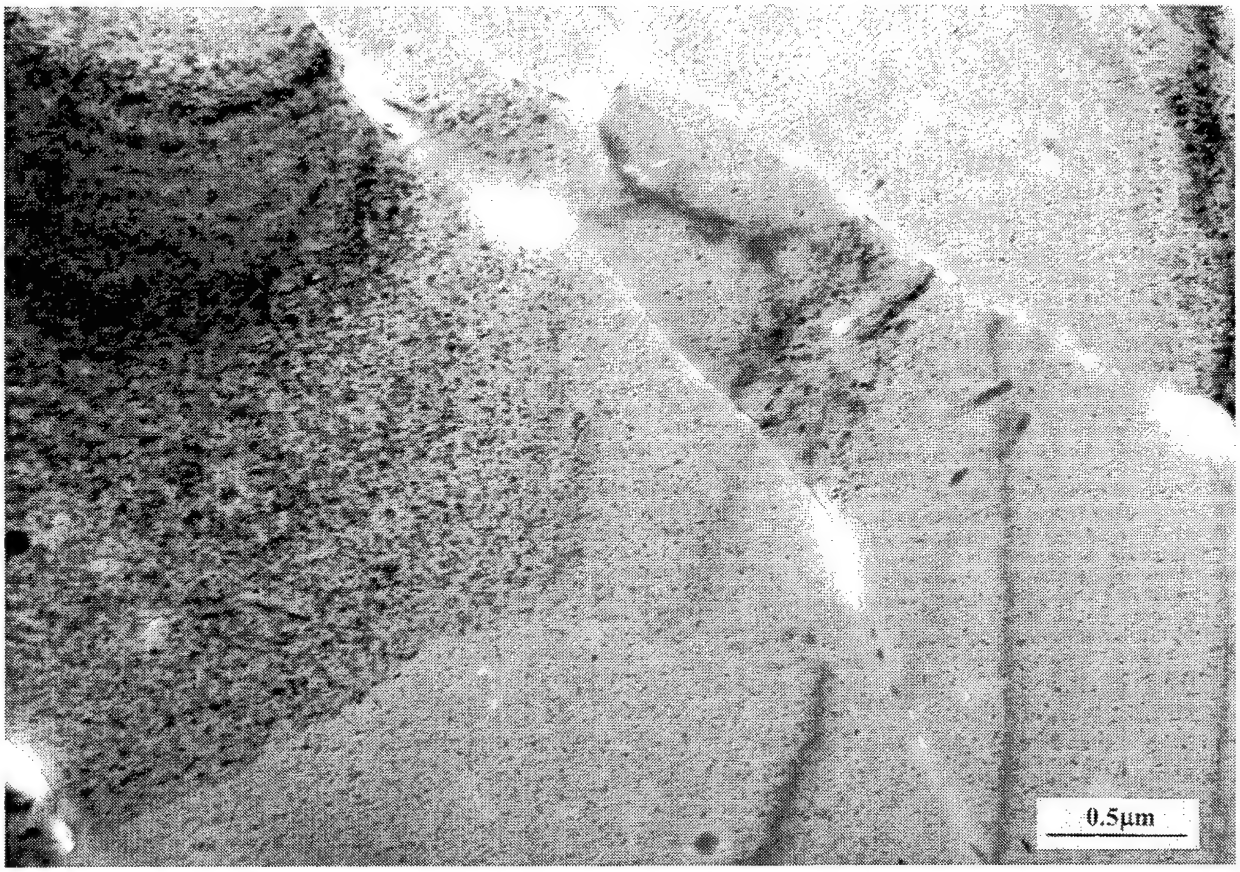

Figure A-10: TEM Micrograph of Overaged Specimen

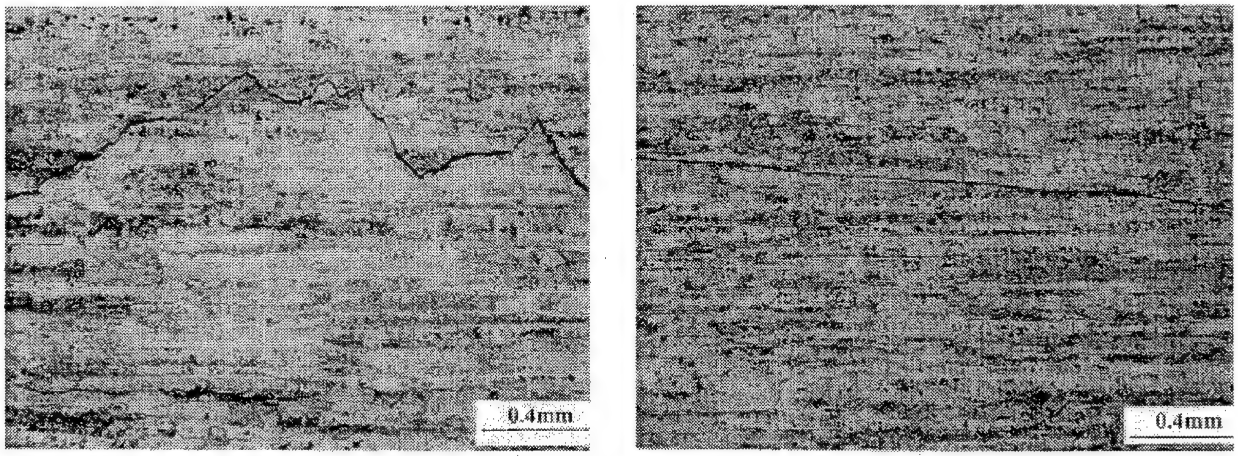

(a) Underaged, R=0.1 (b) Overaged, R=0.2

Figure A-11: Fatigue Crack Paths in Underaged and Overaged Specimens

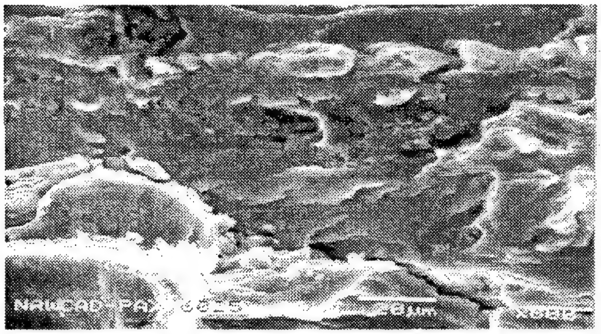

R=0.1, ΔK=7.47 Mpa·m$^{1/2}$
K_{max} = 8.24 Mpa·m$^{1/2}$

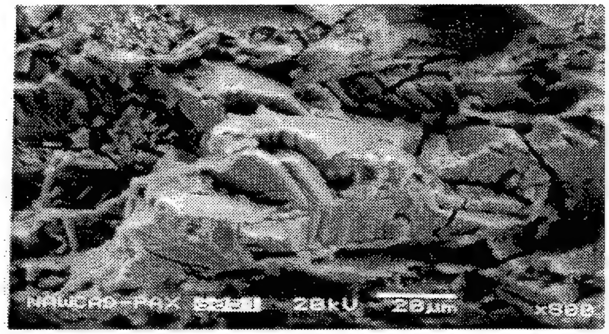

R=0.85, ΔK= 4.95 Mpa·m$^{1/2}$
K_{max} = 32.97 Mpa·m$^{1/2}$

(a) Underaged

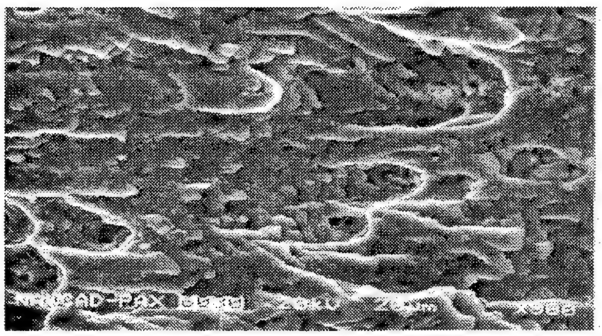

R=0.1, ΔK= 5.50 Mpa·m$^{1/2}$
K_{max} = 6.04 Mpa·m$^{1/2}$

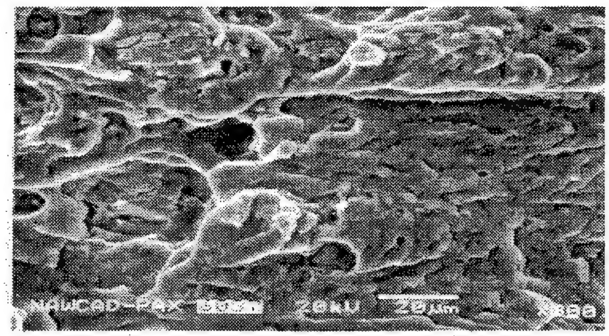

R=0.85, ΔK= 2.97 Mpa·m $^{1/2}$
K_{max} = 19.78 Mpa·m$^{1/2}$

(b) Overaged

Figure A-12: SEM Fractographs of Underaged and Overaged Specimens at da/dN = (7.6~12.7) X 10^{-10} m/Cycle

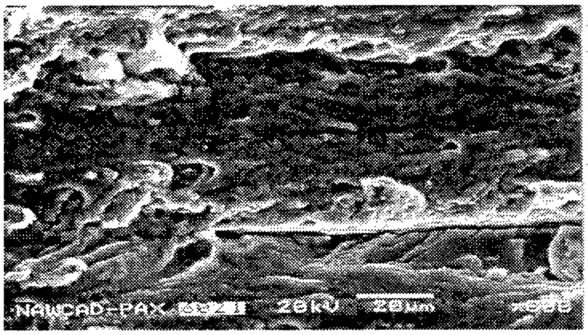

R=0.1, ΔK= 6.70 Mpa·m$^{1/2}$
K_{max} = 7.47 Mpa·m$^{1/2}$

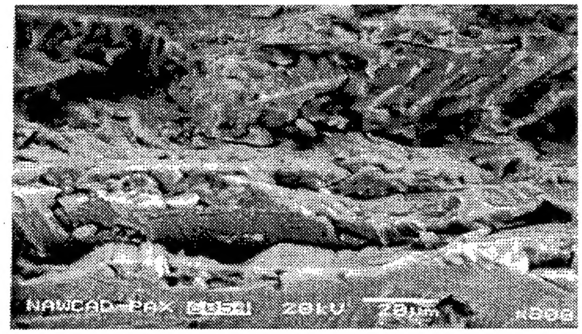

R=0.85, ΔK= 4.62 Mpa·m$^{1/2}$
K_{max} = 30.77 Mpa·m$^{1/2}$

(a) Underaged

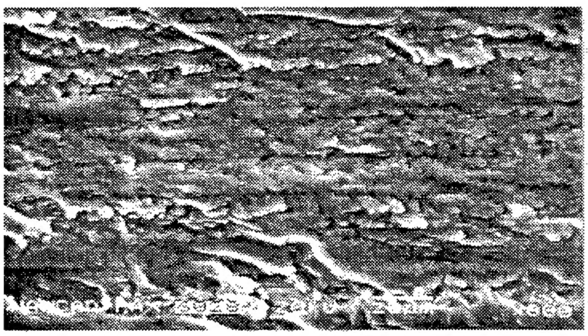

R=0.1, ΔK= 6.81 Mpa·m$^{1/2}$
K_{max} = 7.58 Mpa·m$^{1/2}$

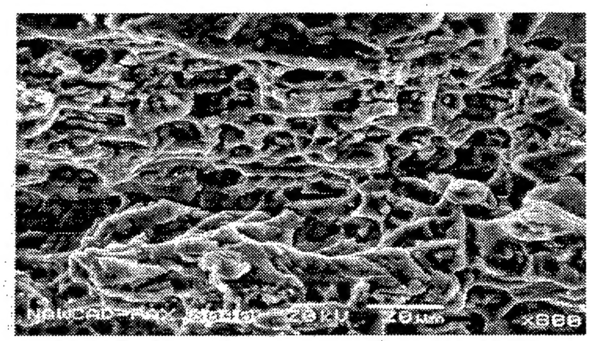

R=0.85, ΔK= 2.64 Mpa·m $^{1/2}$
K_{max} = 17.58 Mpa·m$^{1/2}$

(b) Overaged

Figure A-13: SEM Fractographs of Underaged and Overaged Specimens
at da/dN = (1.0~1.5) X 10^{-10} m/Cycle

DISTRIBUTION:

Army Materials Command (AMCCE-BD) 5001 Eisenhower Ave., Alexandria, VA 22333	(1)
NAVAIRSYSCOM (AIR-4.3.4), Bldg. 2188 48066 Shaw Road, Patuxent River, MD 20670-1908	(1)
NAVAIRSYSCOM (AIR-4.11), Bldg. 304, Room 102 22541 Millstone Road, Patuxent River, MD 20670-1606	(1)
NAVSEASYSCOM 2531 Jefferson Davis Highway, Arlington, VA 22242	(1)
Naval Research Laboratory 4555 Overlook Ave. S.W., Washington, DC 20375-5000	(1)
NAVAIRDEPOT (Code 4.3.4) Naval Air Station, Jacksonville, FL 32212	(1)
NAVAIRDEPOT North Island (Code 4.3.4) 222 East Ave., San Diego, CA 92135-5112	(1)
NAVAIRWARCENACDIV Lakehurst Lakehurst, NJ 08733-5000	(1)
Office of Naval Research (Dr. A. K. Vasudevan) Ballston Centre Tower One 800 North Quincy Street, Arlington, VA 22217-5660	(1)
NAVAIRWARCENACDIV (4.3.4.1), Bldg. 2188, R203C-B1 48066 Shaw Road, Patuxent River, MD 20670-1908	(1)
NAVAIRWARCENACDIV (4.3.4.2), Bldg. 2188 48066 Shaw Road, Patuxent River, MD 20670-1908	(50)
NAVAIRWARCENACDIV (4.3.4.3), Bldg. 2188, R203F 48066 Shaw Road, Patuxent River, MD 20670-1908	(1)
NAVAIRWARCENACDIV (7.2.5.1), Bldg. 405, Room 108 22133 Arnold Circle, Patuxent River, MD 20670-1551	(1)
NAVAIRWARCENACDIV (55TW01A), Bldg. 304, Room 200 22541 Millstone Road, Patuxent River, MD 20670-1606	(1)
DTIC 8725 John J. Kingman Road, Suite 0944, Ft. Belvoir, VA 22060-6218	(1)